NASA TECHNICAL NOTE

NASA TN D-1862

c.1

NASA TN D-1862

RADIATION DOSIMETRY ABOARD THE SPACECRAFT OF THE EIGHTH MERCURY-ATLAS MISSION (MA-8)

by Carlos S. Warren and William L. Gill
Manned Spacecraft Center
Houston, Tex.

NATIONAL AERONAUTICS AND SPACE ADMINISTRATION • WASHINGTON, D. C. • AUGUST 1964

RADIATION DOSIMETRY ABOARD THE SPACECRAFT OF THE EIGHTH MERCURY-ATLAS MISSION (MA-8)

By Carlos S. Warren and William L. Gill

Manned Spacecraft Center
Houston, Tex.

NATIONAL AERONAUTICS AND SPACE ADMINISTRATION

For sale by the Office of Technical Services, Department of Commerce,
Washington, D.C. 20230 -- Price $0.50

RADIATION DOSIMETRY ABOARD THE SPACECRAFT OF THE EIGHTH MERCURY-ATLAS MISSION (MA-8)

By Carlos S. Warren and William L. Gill

SUMMARY

The creation of an artifically trapped electron belt by a high-altitude nuclear explosion on July 9, 1962, made it necessary to place radiation dosimeters aboard the spacecraft used in the eighth Mercury-Atlas mission (MA-8) on October 3, 1962, since the last three orbits passed through a magnetic field anomaly where the belt exists at Mercury flight altitudes. Dosimeters on board the spacecraft of the MA-8 mission were a self-indicating ionization chamber, lithium fluoride thermoluminescent detectors, and nuclear emulsions. The measurements indicated that the astronaut received less than 30 millirads, body surface dose.

INTRODUCTION

On July 9, 1962, an international AGIWARN message quoted the following: "A megaton yield range device was detonated in the ionosphere at an altitude of hundreds of kilometers in the vicinity of Johnston Island in the Pacific at 0900 U.T. on 9 July 1962." Several hours thereafter, geiger counters on the Injun I satellite recorded an increase of up to a hundred times the normal count rate of radiation as the satellite passed through the lower Van Allen belt (ref. 1).

The increase in counting rates was attributed to energetic electrons emitted by the radioactive decay of fission nuclei. These electrons presumably have a differential number energy spectrum, shown in figure 1, approximated by $C \exp(-0.575E - 0.055E^2)$ for the range $1 \leq E \leq 7$, where E is the electron energy in Mev and C is a constant (ref. 2). Some of the electrons emitted were injected at such pitch angles to the geomagnetic field vector that they were trapped, executing oscillatory motion in latitude along magnetic lines and drifting eastward in longitude. The net effect was the formation of an artificial electron belt surrounding the earth.

Although the main portion of the belt is well above the altitude of manned orbital space flights, an anomaly centered in the region of 5° W. longitude, 45° S. latitude permitted the trapped electrons to dip as low as 100 kilometers, according to Dr. W. N. Hess of NASA Goddard Space Flight Center. Since the path of the MA-8 mission passed through this region on the last three orbits, detectors were placed on board the spacecraft to assess the dose accumulated by Astronaut Walter M. Schirra, Jr., from the artifically trapped electrons and the Van Allen belt particles. This paper describes the dosimetry used and presents the results of the measurements.

SYMBOLS

E	electron energy, Mev
E_i	i^{th} electron energy increment
$J\left(\frac{\pi}{2}\right)$	total electrons of fission spectrum normally incident on exterior of hatch cover, e/cm^2
$J\left(\frac{\pi}{2}, x\right)$	normally incident electrons of the fission spectrum attenuated through x thickness of titanium, e/cm^2
$N\left(E_i\right)$	fraction of total electrons in i^{th} group
Q	total charge per unit time in electron beam
$Q_{A \text{ or } B}$	charge accumulated by blocks A or B
R	electron range
R_c	response of ion chamber to fission electrons
$R\left(E_i\right)$	average response of ion chamber to i^{th} energy group
x	shield thickness, g/cm^2
λ	electron backscatter coefficient
ω	fraction of total reflection solid angle that is subtended by block B

DOSIMETER DESCRIPTION

Shown in the photograph in figure 2 are the dosimeters carried on the MA-8 flight, five thermoluminescent dosimeters and a Bendix self-indicating ionization chamber, model 866, which had a range of 0 to 1 roentgen. The ion chamber wrapped in Velcro was placed on the interior of the egress hatch cover (fig. 3). The astronaut read the ion chamber after each orbital pass through the region of interest and the reading was recorded on tape.

Figures 4 and 5 show the placement of the five thermoluminescent dosimeters (TLD) over the eyes, on the chest, and on the interior thigh of the pilot. These detectors were furnished to NASA by the Los Alamos Scientific

Laboratory, New Mexico. Calibration of the dosimeters to fission decay electrons, as well as the reading of the detectors after the mission, was done by LASL.

The MA-8 spacecraft also contained two emulsion packs furnished by Dr. H. J. Schaefer of U. S. Naval School of Aviation Medicine, Pensacola, Florida, to monitor the interior proton dose. These packs, each of which contained a beta-gamma sensitive film, were located on each side of the instrument console.

The Bendix ionization chamber was designed for monitoring primarily X- and gamma-radiation. It was calibrated at the factory and guaranteed to an accuracy of ±10 percent of full-scale reading for dose rates up to 6×10^5 roentgens per hour, independent of incident gamma spectra. However, it was not expected that the instrument would show the same efficiency to electrons, mainly because the dosimeter wall thickness (≈ 250 mg/cm^2) significantly attenuates electrons having energies less than several Mev.

The ion chamber had the advantage of being readily obtainable, inherently rugged, and completely self-contained, in that once it was charged, it required no power supply or electronic read-out. In addition, it had the capability of withstanding the reduced atmospheric pressure of 5 psi within the spacecraft cabin without leakage, and gave the astronaut a real-time estimate of his dose.

RESULTS AND ANALYSIS

The reading of the ionization chamber was reported by the astronaut after the last pass through the anomaly to be approximately 60 milliroentgens. Calibration of the ionization chamber to a Co^{60} gamma-ray source established that the average detector reading was within 1 percent of the true dose, with a standard deviation of 3 percent. It is estimated that a reading error of ±10 milliroentgens could have been made, which represents a larger error of ±17 percent. The gamma-equivalent dose received by the ionization chamber was taken to be 60 ± 10 milliroentgens.

The wall thickness of the aluminum chamber is approximately equivalent to 0.2 to 0.4 g/cm^2 of tissue if the ionizing particles are electrons or protons. The emulsions flown on the MA-8 flight show that protons were present within the spacecraft cabin.

In order to estimate the electron energy that will penetrate the egress hatch cover, approximately 0.6 g/cm^2 of the wall of the ion chamber, the empirical formula of reference 3, relating electron range and energy for particles from 1 to 20 Mev was used.

$$R = 0.530E - 0.106 \text{ g/cm}^2 \qquad (1)$$

Equation (1) gives a minimum energy of 1.3 Mev that will penetrate the hatch cover, and 1.8 Mev that will penetrate both the hatch cover and ion chamber. This was borne out experimentally by exposing the ion chamber and hatch cover to several energies of monoenergetic electron beams. Details of the exposure are covered in appendix A. Approximately 65 percent of the artificial belt electrons have energies less than 1.3 Mev (see fig. 1) and do not penetrate the hatch cover, which is the least-shielded region of the spacecraft. The rest of the spacecraft is more heavily shielded, which allows only a small percentage of the electrons to penetrate to the astronaut.

Two packages of nuclear emulsions were flown on the MA-8 mission. One package was mounted behind the right (astronaut's) instrument console, at the relative position coordinates of $x = 22.3$ inches, $y = 0.7$ inches, and $z = 32.6$ inches, where x corresponds to the spacecraft pitch-axis, y the yaw-axis, and z the roll-axis. The distances x and y are measured from vehicle centerline, and z from the heat shield. The other emulsion package was mounted behind the left console at relative positions of $x = 17.4$ inches, $y = 13.5$ inches, and $z = 35.8$ inches. The emulsion packs were wrapped in paper and epoxy which had a thickness of a few tenths of g/cm^2.

The proton dose measured by the emulsions was determined by the grain-counting method. Above 30 Mev, the ionized grains along the proton's path is a good measurement of the linear energy transfer (LET) and, therefore, the dose. Tissue dose is found by using a stopping power ratio of 2.33 of emulsion to tissue. Below 30 Mev, grain density becomes a weak function of LET because of grain saturation. The tracks that fall in this interval are treated by assuming no tracks at zero energy and a differential N/E - Spectrum of constant slope in the zero to 30-Mev interval. The less than 30 Mev particles are distributed into 5-Mev-wide intervals according to the N/E Spectrum.

The proton dose measured at the emulsion locations, when corrected for background from a sea-level control emulsion, was 22 millirads at the right console, and 7 millirads at the left console. Table I summarizes the emulsion measurements.

It is interesting to note that the proton dose varied by more than a factor of three between the two locations. This presumably is a result of uneven distributions of local absorbing matter, which admitted low-energy protons to the emulsion on the right console, but did not admit then to the other emulsion.

Beta-gamma sensitive film was also included in the emulsion packs. The film, which is examined for exposure by densitometric means, recorded only a few milliroentgens of gamma-equivalent dose, bearing out the deduction that few electrons penetrated the spacecraft structure.

The LASL thermoluminescent dosimeters were placed at various locations on the astronaut (fig. 4) to monitor the radiation dose received, and, if possible, record the variation in dose between locations. However, the thermoluminescent dosimeters had a dose threshold of approximately 30 millirads which was not exceeded in any of the four locations.

CONCLUSIONS

Dose measurements on the astronaut during the eighth Mercury-Atlas mission (MA-8) from thermoluminescent detectors established that the astronaut received less than 30 millirads, body surface dose.

Dose measurements from nuclear emulsions and film badges located behind the left and right instrument consoles and from an ionization chamber attached to the egress hatch cover interior established the following:

(a) A proton dose of 22 millirads was recorded behind the right console and 7 millirads behind the left console.

(b) Electron-sensitive films at the emulsion locations recorded only a few milliroentgens, gamma-equivalent dose, which indicated that few electrons penetrated to those locations.

(c) The ionization chamber, located in the most exposed portion of the vehicle, recorded 60 ± 10 milliroentgens, gamma-equivalent dose.

Therefore, it is concluded that the artificial electron belt created by the July 9, 1962, nuclear detonation presented no problem to the MA-8 mission, and the overall radiation dose experienced by the astronaut was small.

Manned Spacecraft Center
National Aeronautics and Space Administration
Houston, Texas, March 31, 1964

APPENDIX A

CALIBRATION TO ELECTRONS

Once the efficiency of the ion chamber to gammas was established, it was necessary to measure its response to electrons in order to interpret the scale reading in terms of physical dose. Accordingly, an experiment was designed using the linear electron accelerator (LINAC) of General Atomics, San Diego, California, as the source of the energetic electrons.

Geometry

Throughout the flight of the eighth Mercury-Atlas mission (MA-8) the ionization chamber was located on the inside wall of the egress hatch cover attached by means of Velcro tape. An attempt was made to duplicate the geometry experimentally and thereby determine the detector response to the ambient space radiation present. The experimental geometry of the exposure is shown in figure 6. The energies of the incident electrons were 3.0, 5.5, and 10.0 Mev. The beam was monitored by collecting the charge on an aluminum block. Beam spread at the exposure distance was such that no fall-off of intensity could be detected within a few feet to the side of the beam center; hence, the beam was monitored simultaneously with dosimeter exposure.

Corrections Applied to the Beam Monitor

To prevent additional charge on the monitor from being picked up from air ionization, the block was insulated and wrapped in grounded aluminum foil. Backscattering from the monitor block was measured by taking the charge off an identical block placed at 45° to the monitor and out of the beam, as shown in figure 7.

The backscatter coefficient λ was calculated as follows:

Let

Q = total charge per unit time in the electron beam

Q_A = charge on block A in the beam

Q_B = charge on block B

ω = fraction of total reflection solid angle subtended by block B

Then

$$Q_A = (1 - \lambda)Q \tag{A1}$$

$$
\begin{aligned}
Q_B &= (1 - \lambda)\,\lambda Q \omega \\
&= (1 - \lambda)\,\lambda \omega \frac{Q_A}{1 - \lambda}
\end{aligned}
\tag{A2}
$$

or

$$\lambda = \frac{Q_B}{Q_A} \frac{1}{\omega} \tag{A3}$$

By substituting the values obtained at $E = 3.0$ Mev a value of λ of 0.27 was obtained.

Response to the Artificial Belt Spectrum

Figure 8 shows the efficiency of the ion chamber on the hatch interior as a function of incident electron energy. The electrons are normally incident on the hatch exterior. The response of the dosimeter normalized to the artificial belt spectrum is shown in table II. Summation of the relative i^{th} responses indicates that the response of the ion chamber on the spacecraft of the MA-8 to the electron current incident on the hatch cover was

$$R_c = 3.2 \times 10^{-10} \; J\left(\frac{\pi}{2}\right) \tag{A4}$$

where $J\left(\frac{\pi}{2}\right)$ is the number of electrons of the fission spectrum normally incident on the spacecraft hatch cover.

In addition to the measurement expressed by equation (A4), dosimeter readings were taken behind several other thicknesses of the spacecraft hatch during calibration. These data indicate that the response of the ion chamber as a function of hatch thickness in grams per square centimeter of titanium, when normalized to the spectrum shown in figure 1, may be expressed by

$$R_c = K \exp(-1.9x)\; J\left(\frac{\pi}{2}\right) \tag{A5}$$

where K is a constant and x is the thickness.

This relationship is shown in figure 9. Comparison of equations (A4) and (A5) indicate that the attenuation of normally incident fission electrons can be expressed by

$$J\left(\frac{\pi}{2},\, x\right) = J\left(\frac{\pi}{2}\right) \exp\,(-1.9x) \tag{A6}$$

APPENDIX B

CALIBRATION TO GAMMA RAYS

The ion chambers that successfully passed the flight qualification tests were calibrated with Co^{60} gamma rays to determine their absolute efficiency of measuring dose with respect to scale reading. The calibration took place at the School of Aerospace Medicine, Brooks Air Force Base, San Antonio, Texas, utilizing facilities loaned NASA by Dr. George Crawford.

Although an ion chamber having the range of 0 to 1 rad was used to monitor the MA-8 flight, it was necessary to gamma-calibrate ion chambers of ranges 0 to 1 rad and 0 to 100 rads because the electron accelerator used for the calibration produced such high dose rates that work was prohibited except with the 100 rad chambers. However, when combined with a gamma cross-calibration, this method adequately determines the efficiency of the 1 rad chambers to electrons, since the basic construction of the two dosimeters is identical, except in the value of the capacitor.

The results of the calibration showed the flight item had a two-standard-deviation limit of 5.7 percent, which is well within the manufacturer's specifications.

REFERENCES

1. O'Brien, B. J., Laughlin, C. D., and Van Allen, J. A.: Preliminary Study of the Geomagnetically-Trapped Radiation Produced by a High-Altitude Nuclear Explosion on July 9, 1962. Reprint from Nature (London) vol. 195, no. 4845, Sept. 8, 1962, pp. 939-943.

2. Carter, R. E., Reines, F., Wagner, J. J., and Wyman, M. E.: Free Antineutrino Absorption Cross Section II. Expected Cross Section From Measurements of Fission Fragment Electron Spectrum. Phys. Rev. 113, 1959, pp. 280-286.

3. Katz, L., and Penfold, A. S.: Range-Energy Relations for Electrons and the Determination of Beta-Ray End-Point Energies by Absorption. Review Modern Physics, vol. 24, no. 1, Jan. 1952, pp. 28-44.

TABLE I. - RESULTS FROM EMULSION USED ON MA-8 MISSION

Grains per 100 MICRA	Proton mean kinetic energy, MEV	Tissue doses, mrad		
		Left console emulsion	Right console emulsion	Sea-level control
50	363	0.18	0.21	0.22
50 to 70	164	.72	.47	.62
70 to 90	133	1.61	1.04	.62
90 to 110	97	2.09	.75	.91
110 to 130	62	1.48	2.42	.55
130 to 150	31	1.36	3.16	.63
>150	<30	4.12	18.41	1.17
TOTAL		11.56	26.46	4.72

TABLE II. - RESPONSE OF THE ION CHAMBER R_c BEHIND THE HATCH

$$\left[\frac{R_c}{J\left(\frac{\pi}{2}\right)} = \frac{\sum N(E_i)\,R(E_i)}{J\left(\frac{\pi}{2}\right)} = 3.2 \times 10^{-10} \right]$$

E_i	$N(E_i)$	$\frac{R(E_i)}{J\left(\frac{\pi}{2}\right)}$, $\frac{1}{e/cm^2}$	$\frac{N(E_i)\,R(E_i)}{J\left(\frac{\pi}{2}\right)}$
<2.0	0.809	0	0
2.0 to 2.5	.068	2.9×10^{-11}	2.0×10^{-12}
2.5 to 3.0	.047	1.1×10^{-10}	5.2×10^{-12}
3.0 to 3.5	.031	3.6×10^{-10}	1.1×10^{-11}
3.5 to 4.0	.016	1.05×10^{-9}	1.7×10^{-11}
4.0 to 4.5	.010	2.50×10^{-9}	2.5×10^{-11}
4.5 to 5.0	.007	5.10×10^{-9}	3.6×10^{-11}
5.0 to 5.5	.004	8.80×10^{-9}	3.5×10^{-11}
5.5 to 6.0	.002	1.35×10^{-8}	2.7×10^{-11}
6.0 to 6.5	.0013	1.80×10^{-8}	2.3×10^{-11}
6.5 to 7.0	.0007	2.20×10^{-8}	1.5×10^{-11}
>7.0	.004	3.0×10^{-8}	1.2×10^{-10}

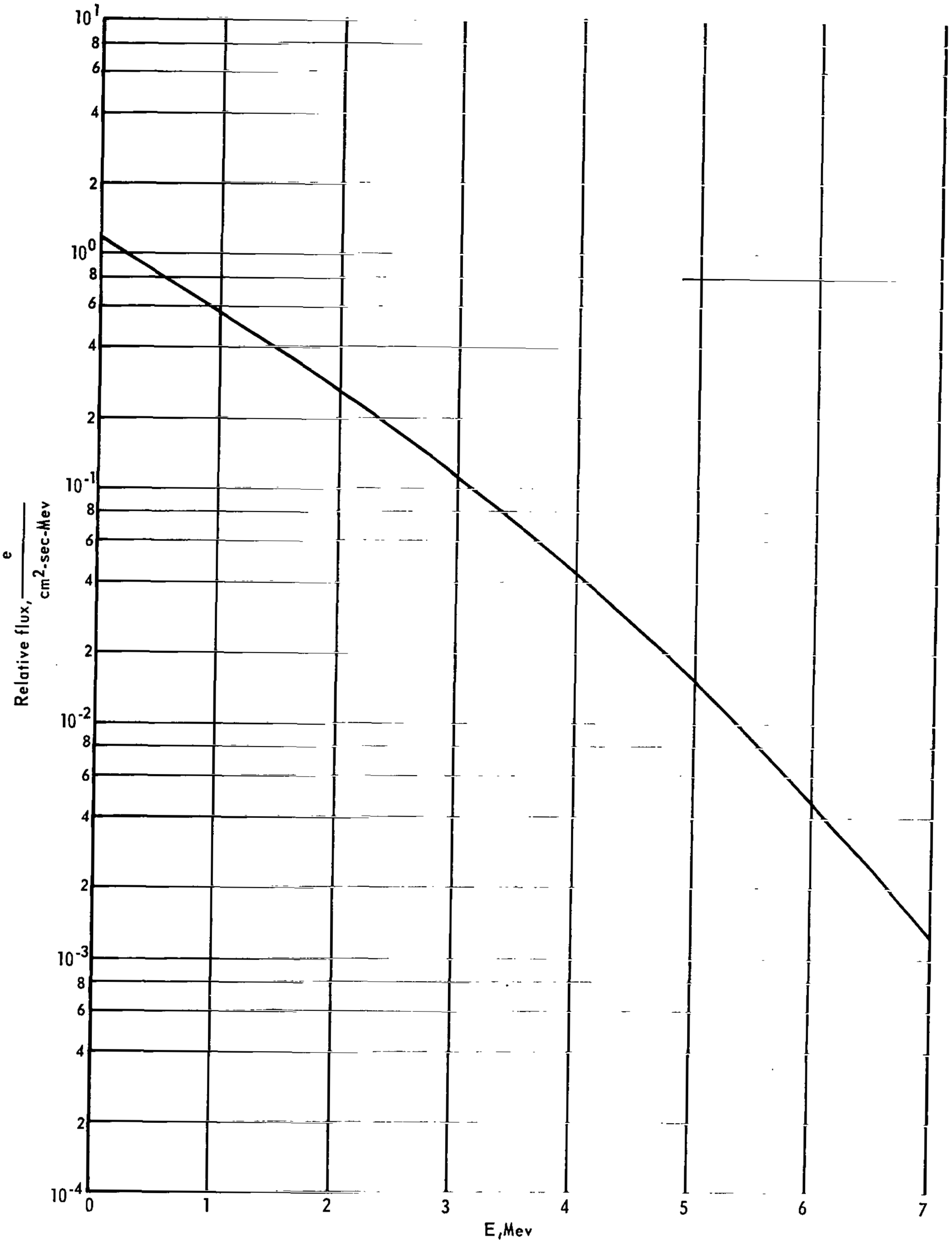

Figure 1.- Artificial belt spectrum.

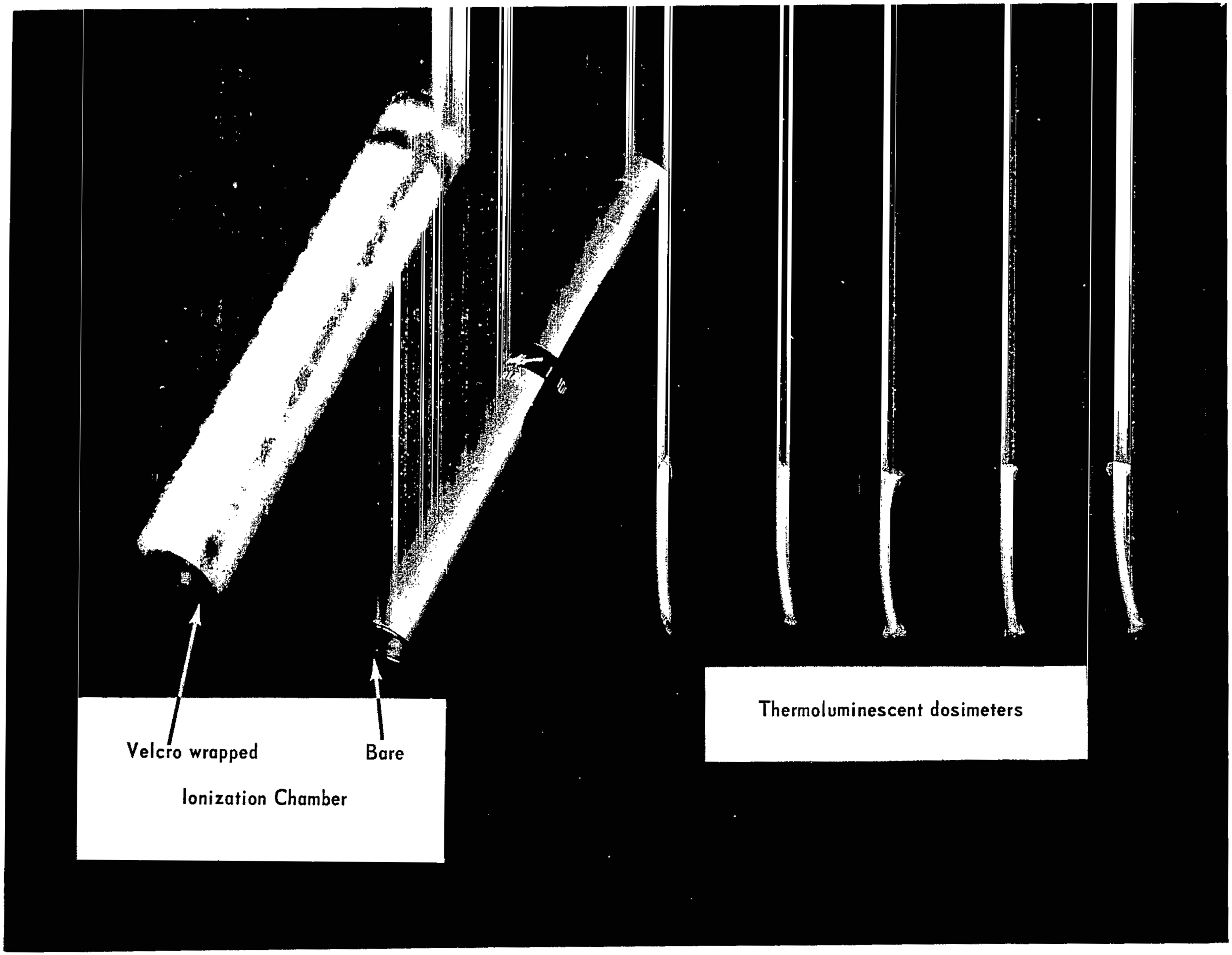

Figure 2.- Photograph of ionization chamber and thermoluminescent dosimeters.

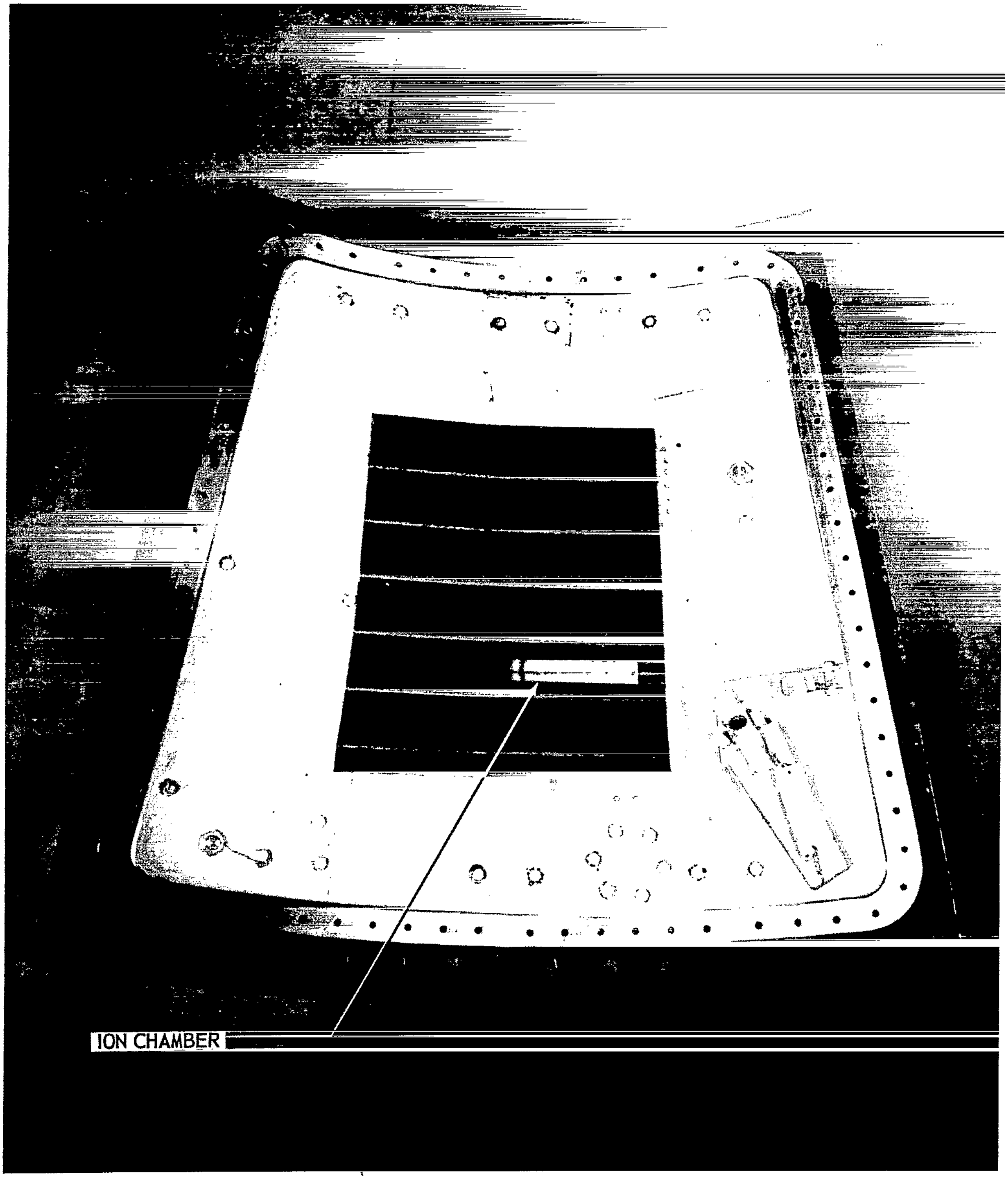

Figure 3.- Ion chamber placement on egress hatch cover.

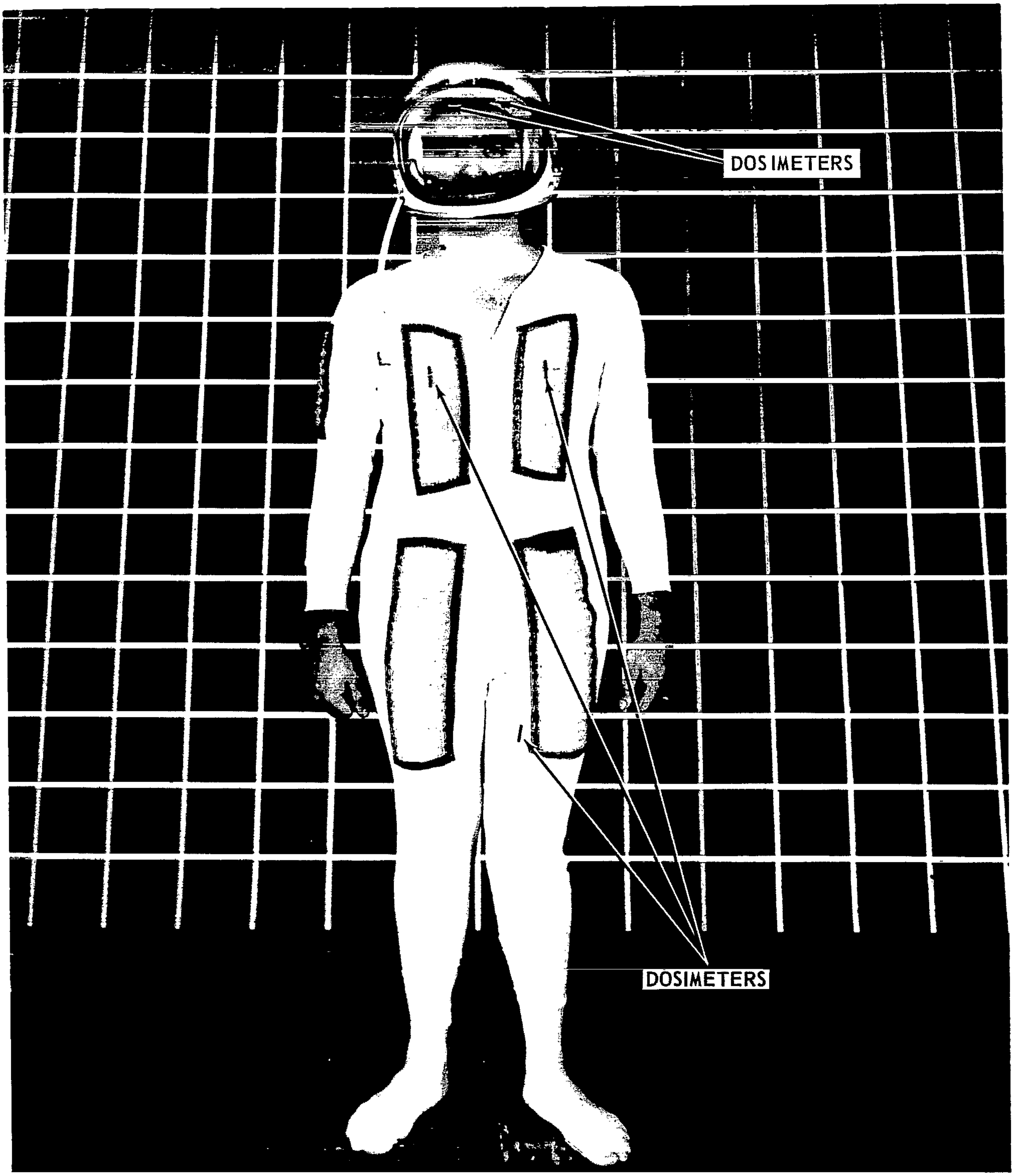

Figure 4.- Placement of thermoluminescent dosimeters on pilot.

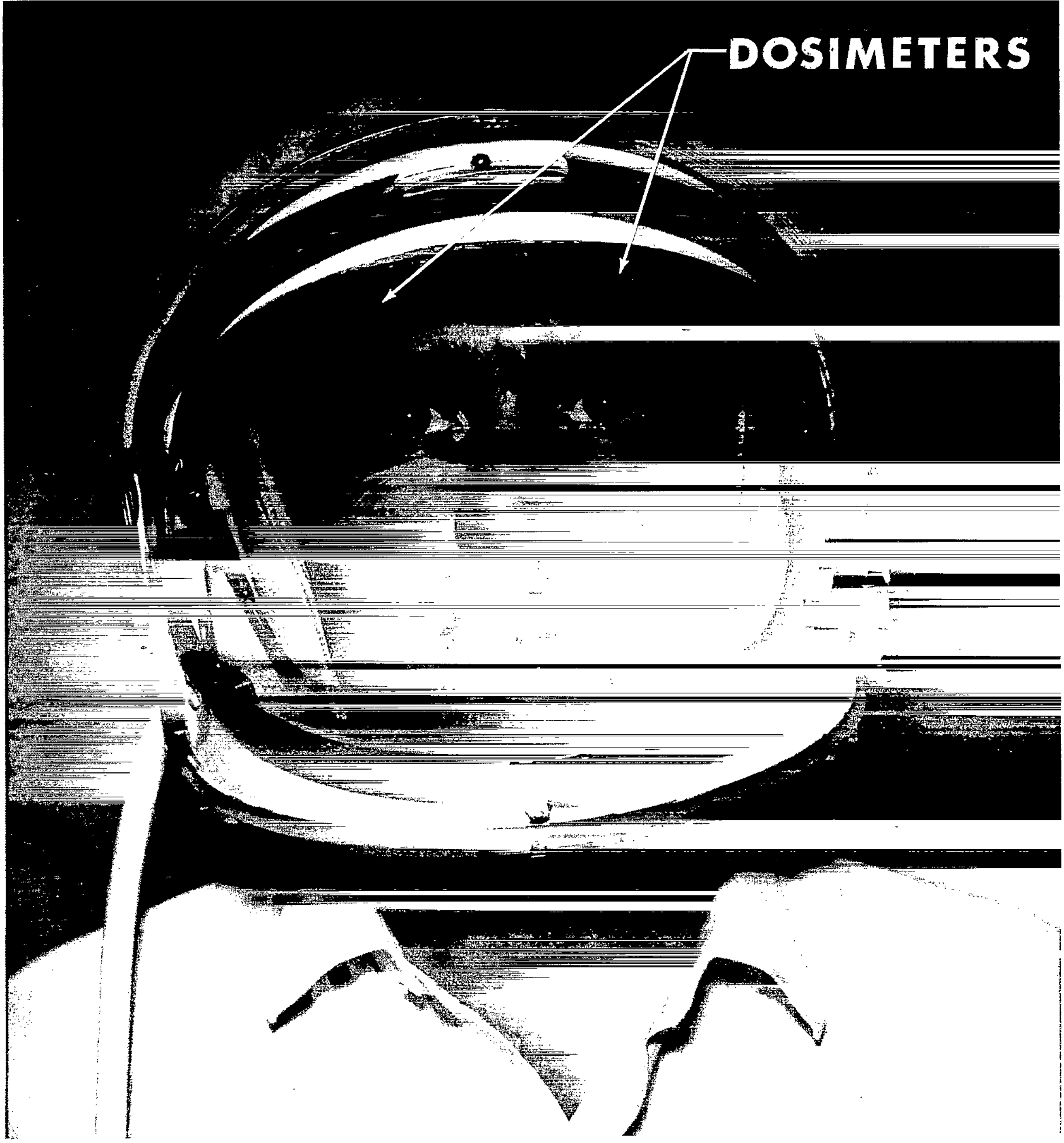

Figure 5.- Placement of thermoluminescent dosimeters on the helmet.

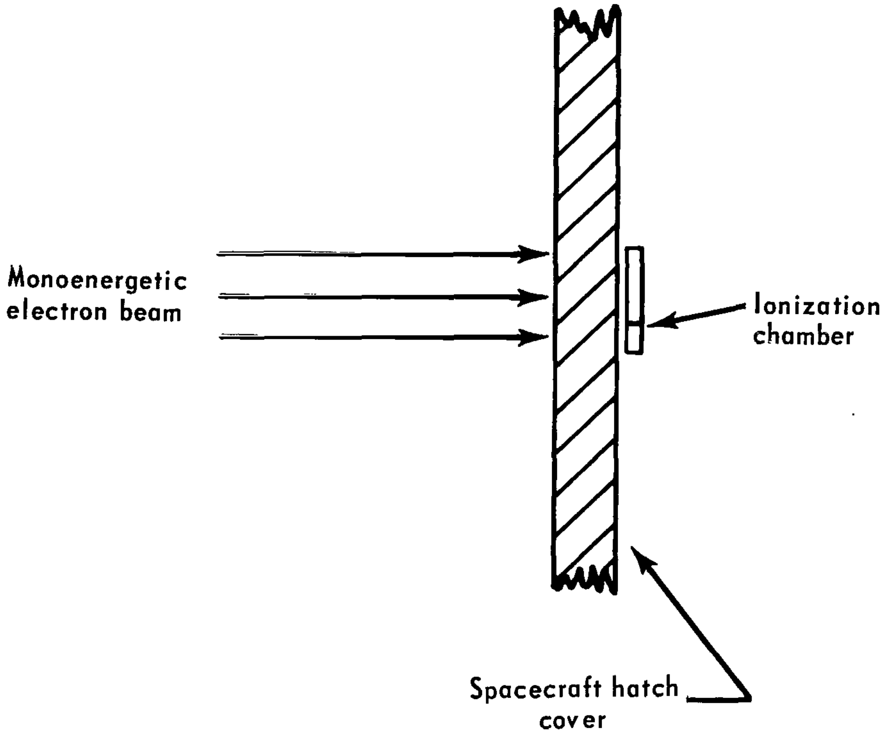

Figure 6.- Calibration behind egress hatch.

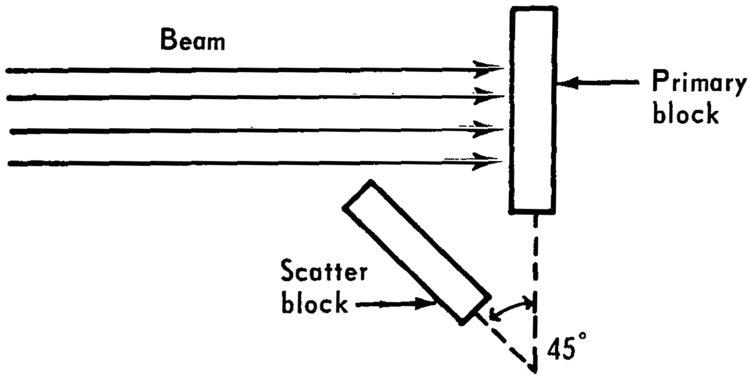

Figure 7.- Backscatter experiment geometry.

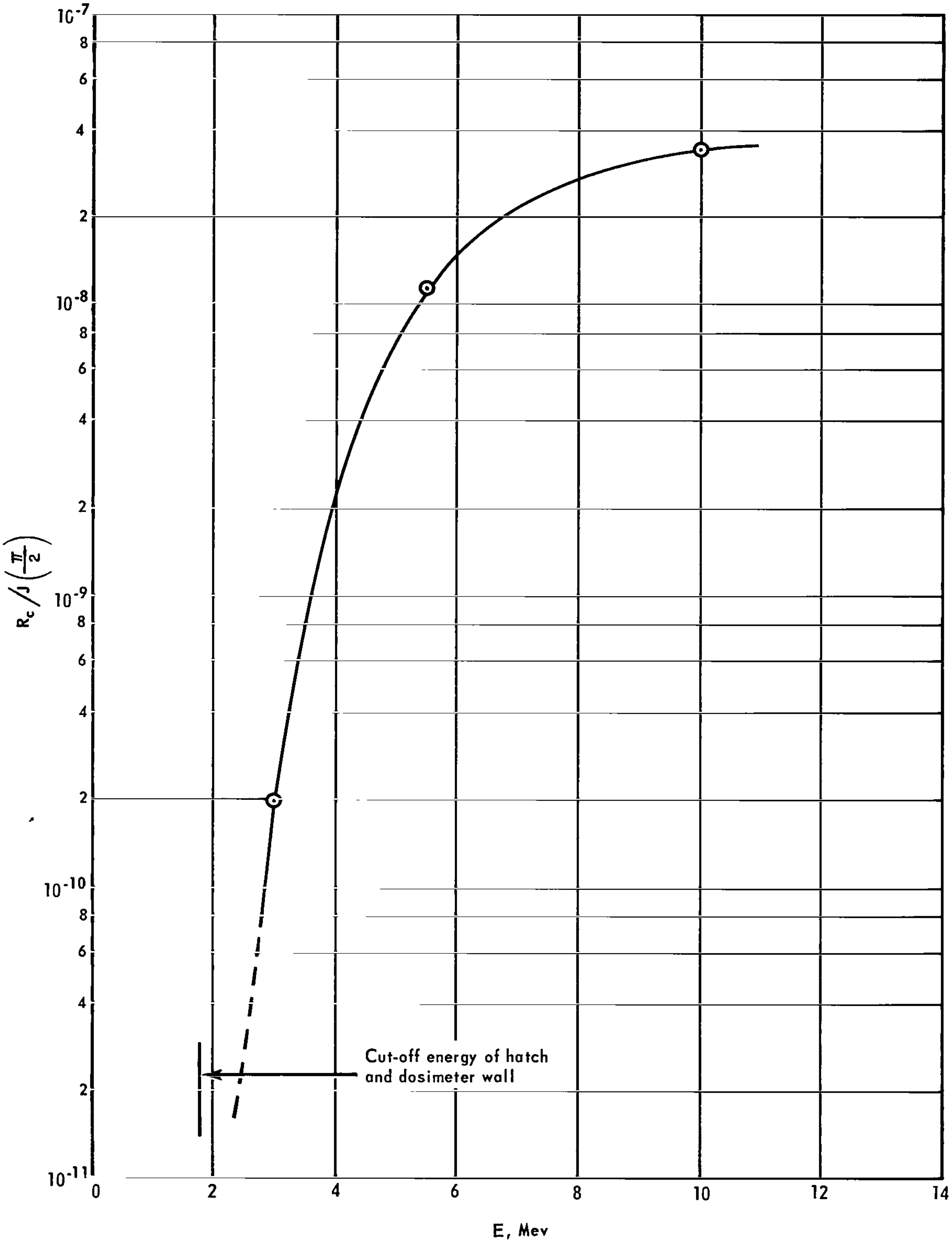

Figure 8.- Ion chamber efficiency behind hatch.

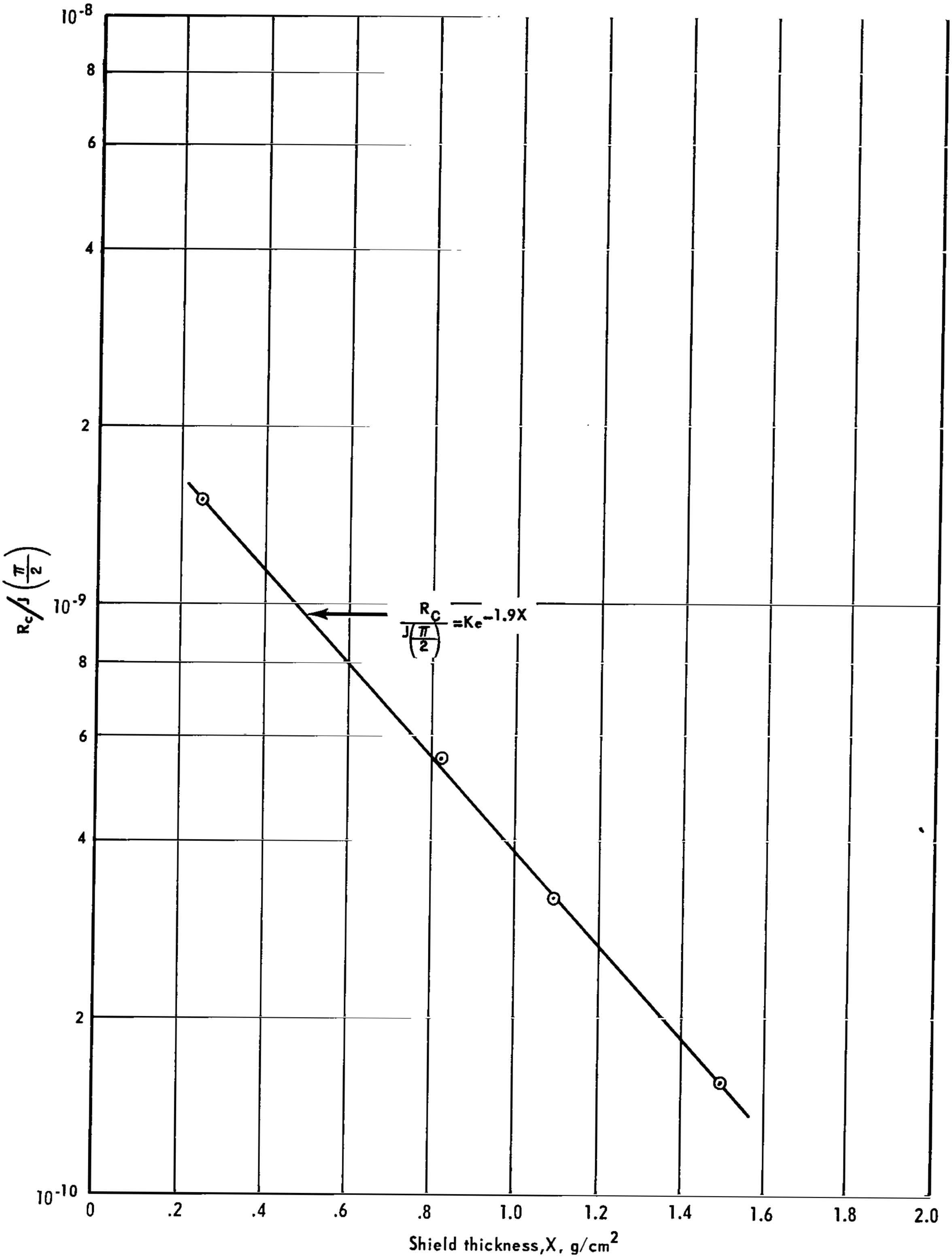

Figure 9.- Response of ion chamber behind varying shield thickness.

NASA-Langley, 1964 S-42

2/16/85

> *"The aeronautical and space activities of the United States shall be conducted so as to contribute . . . to the expansion of human knowledge of phenomena in the atmosphere and space. The Administration shall provide for the widest practicable and appropriate dissemination of information concerning its activities and the results thereof."*
>
> —NATIONAL AERONAUTICS AND SPACE ACT OF 1958

NASA SCIENTIFIC AND TECHNICAL PUBLICATIONS

TECHNICAL REPORTS: Scientific and technical information considered important, complete, and a lasting contribution to existing knowledge.

TECHNICAL NOTES: Information less broad in scope but nevertheless of importance as a contribution to existing knowledge.

TECHNICAL MEMORANDUMS: Information receiving limited distribution because of preliminary data, security classification, or other reasons.

CONTRACTOR REPORTS: Technical information generated in connection with a NASA contract or grant and released under NASA auspices.

TECHNICAL TRANSLATIONS: Information published in a foreign language considered to merit NASA distribution in English.

TECHNICAL REPRINTS: Information derived from NASA activities and initially published in the form of journal articles.

SPECIAL PUBLICATIONS: Information derived from or of value to NASA activities but not necessarily reporting the results of individual NASA-programmed scientific efforts. Publications include conference proceedings, monographs, data compilations, handbooks, sourcebooks, and special bibliographies.

Details on the availability of these publications may be obtained from:

SCIENTIFIC AND TECHNICAL INFORMATION DIVISION
NATIONAL AERONAUTICS AND SPACE ADMINISTRATION
Washington, D.C. 20546